

Acoustic damping in transonic jets by condensed vapour

M. JAESCHKE, W. J. HILLER, G. E. A. MEIER (GÖTTINGEN)

SOME experiments on acoustic damping in a mixture of air and submicroscopic water droplets or ice crystals will be reported. The observed damping can be explained by a mechanism describing condensation and evaporation on droplet or particle surfaces.

Przedstawiono pewne badania eksperymentalne, dotyczące akustycznego tłumienia w mieszaninie powietrza, mikroskopowych kropelek wody i kryształów lodu. Zaobserwowane tłumienie można wytłumaczyć mechanizmem kondensacji i parowania na powierzchniach kropelek lub cząsteczek.

Представлены некоторые экспериментальные исследования, касающиеся акустического затухания в смеси воздуха, микроскопических капель воды и кристаллов льда. Наблюдаемое затухание можно объяснить механизмом конденсации и испарения на поверхностях капель или частиц.

INVESTIGATIONS of transonic jets have shown that the strength of shock and sound waves is considerably reduced as the air moisture content increases [1, 2]. It will be demonstrated that the existing attenuation mechanism is the result of formation and evaporation of water on water droplets or ice crystals.

Figure 1 gives a schematic view of the experimental equipment. Air flows from a balloon through the plane channel in a vacuum chamber. The vertex distance of the laval type

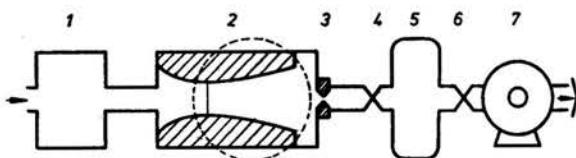


FIG. 1. Sketch of the experimental arrangement.

1. Reservoir (balloon 80m³) for air with variable moisture content.
2. Test section.
3. Throttle valve.
- 4, 6. Quick-acting gate valve.
5. Vacuum chamber.
7. Rotary vane pump 5220m³/h.

nozzle is 5cm and the depth 10cm. The flow is investigated by optical and pressure testing methods.

Figure 2 shows differential interferograms of the flow with different air moisture contents. The air passes through the nozzle from left to right. Downstream of the narrowest cross-section a steady shock wave is formed in the supersonic region of the flow. The boundary layer separates on one side of the contour owing to the pressure jump induced by the shock. This forms a "half" free jet, which is bounded on its upper side by the nozzle contour and on its lower site by a dead water bubble; between this dead water region

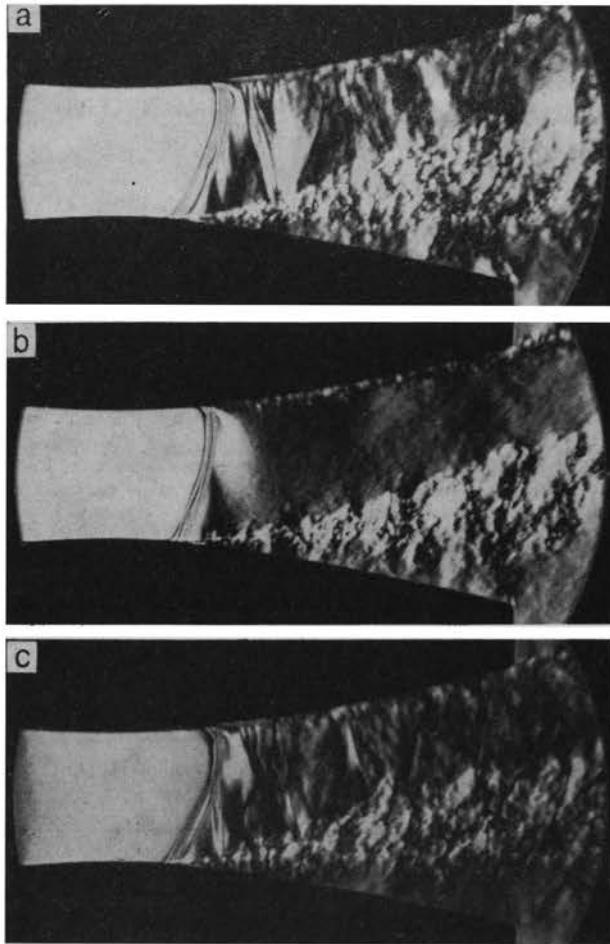


FIG. 2. Differential interferograms of a transonic jet with different relative humidities of moist air φ_0 and temperatures T_0 at rest state. q_0 ist the mixing ratio in g water /kg air.

(a) $\varphi_0 = 9.5\%$, $T_0 = 22^\circ\text{C}$, $q_0 = 1.6$ g/kg,

(b) $\varphi_0 = 26\%$, $T_0 = 22^\circ\text{C}$, $q_0 = 4.3$ g/kg,

(c) $\varphi_0 = 5.1\%$, $T_0 = 50^\circ\text{C}$, $q_0 = 3.9$ g/kg,

and the jet there is a turbulent mixing zone. In the jet density gradients and shock waves are generated during the impingement of the jet on the throttle valve (Figs. 1, 3) and by turbulent pressure fluctuations in the mixing region.

Comparing illustrations (a) and (b), where the initial relative humidity φ_0 of the flow amounts to 9.5% and 26%, respectively, it can easily be seen that the density gradients and shock waves are strongly reduced in the jet at higher air moisture content. In illustration (c) we see strong disturbances similar to those in (a), though the absolute humidity φ_0 is about equally high as in illustration (b). The stagnation temperature is, however, for illustrations (c) sufficiently high, $T_0 = 50^\circ\text{C}$, so that the initial relative humidity is only about 5% and therefore no condensation in the nozzle occurs, as in illustration (a). Further experiments with high initial relative humidity show that no

notable change in flow properties in the jet is caused by condensation during rapid nozzle expansion. This implies that the presence of condensed droplets is essential for the damping mechanism.

With Mach-Zehnder interferograms, Fig. 3, the condensation region in the nozzle, indicated by the annular pattern of the interference fringes, is especially clearly visible. The maximum density amplitudes in the jet fed with dry air are of the order of one half interference fringe. That corresponds to pressure fluctuations of about 10mb or 154dB.

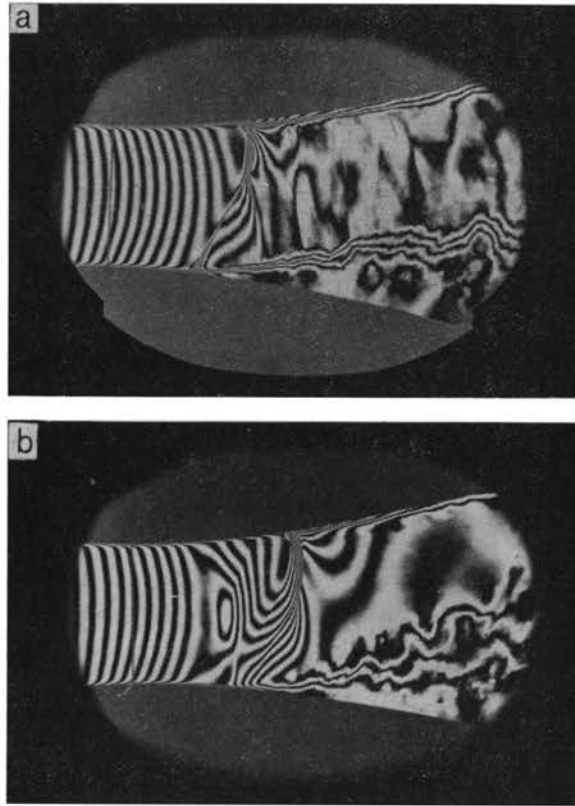


FIG. 3. Mach-Zehnder interferograms of a transonic jet with different relative humidities of moist air φ_0 and temperatures T_0 at rest state; q_0 is the mixing ratio in g water/kg air;

(a) $\varphi_0 = 6.2\%$, $T_0 = 18.9^\circ\text{C}$, $q_0 = 0.9 \text{ g/kg}$,

(b) $\varphi_0 = 60.8\%$, $T_0 = 17.6^\circ\text{C}$, $q_0 = 8 \text{ g/kg}$.

Streak pictures show that these disturbances are moving downstream at a velocity of about 250m/s and upstream at about 100m/s relative to the laboratory system [2, 3].

Investigating the wall pressure fluctuations of the jet with piezoelectric transducers confirms the above results for the strength and propagation velocity of the disturbances. In Fig. 4 the recordings of frequency spectra of the wall pressure fluctuations in the jet are reproduced for two different air humidities. Within the frequency range of 1–25kHz the levels with moist air are lower than with dry air. The amplitudes of the wall pressure fluctuations for the flow with an initial relative humidity of $\varphi_0 \approx 55\%$ are on the average about 8dB smaller than for the flow with dry air of $\varphi_0 \approx 10\%$. At lower frequencies

the levels are about equal, with the exception of frequencies around 300 Hz. These wall pressure fluctuations are generated by oscillating shock waves, and their amplitudes are reduced in the order of 7 dB, the shock waves being considerably stabilized due to the condensation process. At higher frequencies the amplitudes of the wall pressure fluctuations in the jet are continually reduced with growing moisture content, as shown by further investigations with intermediate values of relative humidity around 30% [3].

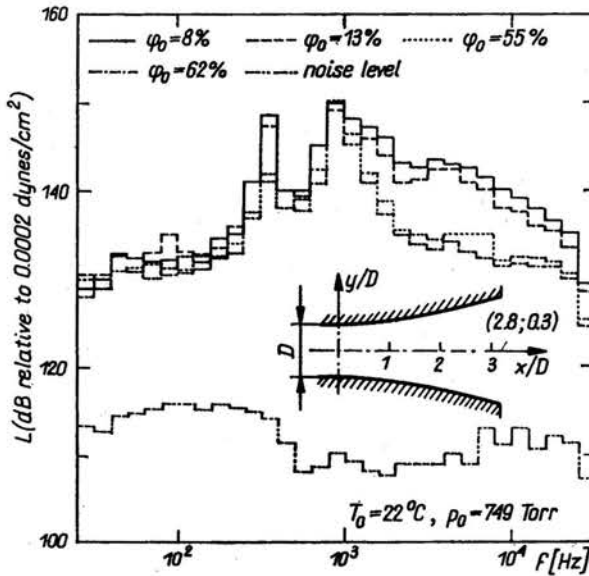


FIG. 4. Third octave frequency spectra of wall pressure fluctuations for different air moisture contents; $D = 5$ cm, the vertex distance of the nozzle.

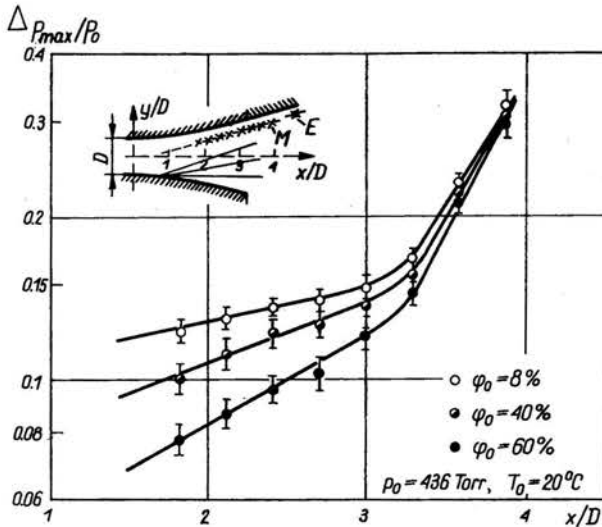


FIG. 5. Decay of upstream-moving, artificial pressure waves for different air moisture contents; E excitation centre, M is the closest measuring station to E , p_0 stagnation pressure.

Artificial disturbances generated by exploding thin copper wires with an electrical discharge at the location E in the jet behave in the same way. Figure 5 shows the decay of the amplitudes of artificial pressure waves in the jet with different initial humidities. As the artificial pressure waves pass along the measuring points in the jet, an increase in pressure occurs above the natural pressure fluctuations. This additional maximum increase is indicated by Δp_{\max} . Adjacent to the excitation centre E and upstream as far as $x/D = 3$, the amplitude of the pressure waves decreases rapidly until they assume rather a character similar to plane waves. The pressure waves in a dry jet also decay due to their geometrical rarefaction. The additional damping in a jet with moist air can be derived from the deviation of the rate of decay between dry and moist air. In this way an amplitude damping coefficient for a relative humidity of 60% was found experimentally to be of the order of 4.3 m^{-1} corresponding to an attenuation of the pressure waves of 37 dB/m.

Table 1. Amplitude attenuation coefficient in the jet with an air moisture content of $\varphi_0 = 60\%$ for

	$[\text{m}^{-1}]$	$[\text{dB m}^{-1}]$
natural disturbances	3 ± 1.3	26 ± 11
artificial pressure waves	4.3 ± 1.5	37 ± 13
artificial density waves	3.8 ± 1.5	33 ± 13

Investigations of these artificial disturbances with a Mach-Zehnder interferometer yield similar values for this additional damping in a moist jet, Table 1. The amplitude damping coefficients for the natural disturbances, which were determined by measuring the decay of the over-all level of the disturbances without any artificial pressure or density waves in the jet, is somewhat lower, of the order of 3 m^{-1} . This smaller decay for the natural disturbances compared to the artificial ones in the jet is reasonable, since the spectra of the natural pressure fluctuations consist mainly of lower frequencies around 1 kHz. These frequencies, however, are less damped than the higher frequencies, which predominantly occur in explosion waves.

The assumptions made for calculating the propagation of sound in a jet will be given below. In addition the theoretical acoustic damping values will be compared with our experimental data⁽¹⁾. Initially, the system consisting of small spherical droplets suspended in a mixture of their vapour and air, is considered to be undisturbed, in equilibrium, when no sound waves are applied. The perturbation of this system by plane acoustic waves causes an exchange of mass, momentum and energy between the droplets and the surrounding gas-mixture. The system does not always reach equilibrium, resulting in attenuation and dispersion of the sound.

To calculate these relaxation processes it is necessary to use the laws for the exchange of mass, momentum and energy between the droplet and the ambient gas. In the continuous region between the droplet surface and its remote surrounding, heat and water diffuse due to gradients of temperature and density. There is also a flow through the surface caused by temperature and density jumps. The diffusion rate of water \dot{m}_1 , for example, is proportional to the droplet radius r and is a function of the temperature and density differences of water vapour between the two locations;

$$(1) \quad \dot{m}_1 \sim rf(\rho_\infty - \rho_r, T_\infty - T_r),$$

⁽¹⁾ More details can be found in [3].

where ρ_∞ is the vapour density and T_∞ is the temperature in the remote surroundings of the droplet, and ρ_r and T_r are the corresponding values on the droplet surface. The exchange of water through the surface \dot{m}_2 , however, is proportional to r^2 ;

$$(2) \quad \dot{m}_2 \sim r^2 g(\rho_r - \rho_s(T_t, r), T_r - T_t),$$

where ρ_r is the actual density and $\rho_s(T_t, r)$ is the saturation density of water on the droplet surface and T_t is the droplet temperature.

The relaxation is determined by the slower of these two processes. For large droplets ($r >$ mean free path l), the non-equilibria in the continuous region are the driving forces [Eq. (1)], whereas the exchange through the surface takes place practically in thermodynamic equilibrium. For this limiting case COLE and DOBBINS [4] and MARBLE and WOOTEN [5] have calculated the relaxation processes. We consider a different case. The mean path of the molecules in the jet is about $5 \cdot 10^{-7}$ m and the droplet size

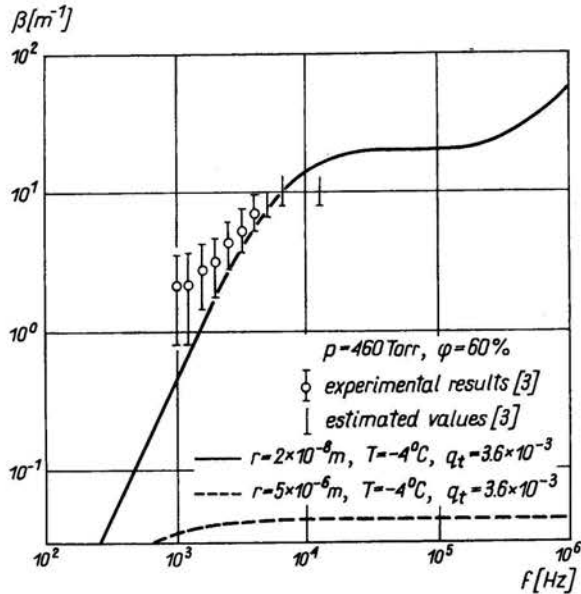


FIG. 6. Attenuation of acoustic energy in a gas mixture with suspended ice particles as a function of frequency. The estimated values are experimentally measured lower limits.

varies from 10^{-8} – $2 \cdot 10^{-8}$ m. These are typical values in rapid nozzle expansions. In this case the non-equilibrium at the surface is relevant [Eq. (2)], and we may assume the system in the continuum region to be almost in equilibrium. The mass, momentum and energy exchange processes at the surface of the droplet in this range of large Knudsen numbers are described using the approach of [6, 7, 8]. Taking into account this behaviour for these processes we can calculate the relaxation processes and obtain a dispersion relation. From this relation we can determine the damping coefficient curve as a function of frequency.

Figure 6 shows calculated curves for the damping of sound waves in a gas mixture at rest with suspended ice particles. The solid line represents the attenuation under

conditions such as are to be found in the jet. The mean value for the particle radii in the jet of $r = 2 \cdot 10^{-8}$ m was calculated by a one-dimensional streamline theory, using experimentally determined pressure and density curves of the nozzle flow. The dashed line represents the attenuation by ice particles with radii of $r = 5 \cdot 10^{-6}$ m, which can also be obtained by means of the COLE and DOBBINS theory [4]. Comparing these two curves in their flat part at about 10^4 Hz, it can easily be seen that the damping by submicroscopic ice particles exceeds the damping on large particles as they are found in clouds by more than three orders of magnitude. The spectral damping coefficients obtained by measuring the decay of the disturbances along their propagation direction upstream in the jet were converted to the attenuation coefficients for a medium at rest. Comparing the damping coefficients obtained experimentally with the calculated coefficient for radii of $r = 2 \cdot 10^{-8}$ m yields good agreement. Comparing an approximate solution by taking into account only the mass and energy exchange on the droplets with the exact dispersion relation, we find that both solutions yield, for radii of $2 \cdot 10^{-8}$ m, identical values for the attenuation below frequencies of about 10^5 Hz. For large droplets, $r = 5 \cdot 10^{-6}$ m, the values coincide only below 10^2 Hz. From these latter results we have to conclude, that the damping observed experimentally in the frequency range of $10^3 - 10^4$ Hz has to be explained exclusively by the formation and condensation of water vapour on particle surfaces and by heat input into this cyclic process, resulting in dissipation of acoustic energy.

References

1. W. J. HILLER, M. JAESCHKE, G. E. A. MEIER, *Einfluß der Luftfeuchtigkeit auf schwache Stoßwellen in schallnahen Freistrahlen*, GAMM Tagung, Delft 1970, ZAMM, 51, T 149, 1971.
2. W. J. HILLER, M. JAESCHKE, G. E. A. MEIER, *The influence of air humidity on pressure and density fluctuations in transonic jets*, J. Sound Vib., 17, 423, 1971.
3. M. JAESCHKE, *Dämpfung von Druck- und Dichteschwankungen in einem schallnahen Freistrahle durch kondensierten Wasserdampf*, Dissertation, Universität Göttingen, 1973; erschienen als Mitteilungen aus dem Max-Planck-Institut für Strömungsforschung und der Aerodynamischen Versuchsanstalt, Nr. 57, 1973.
4. J. E. COLE, R. A. DOBBINGS, *Propagation of sound through atmospheric fog*, J. atmos. Sci., 27, 426, 1970.
5. F. E. MARBLE, D. C. WOOTEN, *Sound attenuation in a condensing vapour*, Phys. Fluids, 13, 2657, 1970.
6. N. A. FUCHS, *The mechanics of aerosols*, Pergamon Press, Oxford 1964.
7. N. A. FUCHS, A. G. SUTUGIN, *Highly dispersed aerosols*, Ann. Arbor. Science Publishers, London 1970.
8. S. W. KANG, *Analysis of condensation droplet growth in rarefied and continuum environments*, AIAA. J., 5, 1288, 1967.

MAX-PLANCK-INSTITUT
FÜR STRÖMUNGSFORSCHUNG.
GÖTTINGEN.

Received October 9, 1973.